Shifted SABR Model: Normal Volatilities

Your Name

March 11, 2025

Contents

1 Exercise 1

a) Implement the shifted SABR model (Hagan et al. "Universal Smiles", 2016) for Swaptions and calibrate its parameters to the market physical Swaption volatility cube.
b) Test the calibration precision with respect to different objective functions (i.e. relative price differences, RMSE volatility, vega-weighted RMSE volatility).
c) Test different optimization methods in terms of calibration precision and performance.
d) Test SABR parameter redundancy.

1.1 Introduction

The **SABR (Stochastic Alpha Beta Rho)** model is one of the most widely used stochastic volatility models in financial markets, particularly for pricing and hedging **interest rate derivatives** such as **Swaptions** and **Caps/Floors**. The model, introduced by Hagan et al. (2002), has gained prominence due to its ability to capture the **volatility smile** observed in market option prices. However, standard SABR formulations assume a lognormal distribution of forward rates, which becomes problematic in low or negative interest rate environments.

To address this, practitioners use the **shifted SABR model**, where the forward rate is adjusted by an additive constant o, ensuring positive values even when interest rates are near or below zero. This modification is particularly relevant in the **post-2008 financial environment**, where central bank policies have driven rates to unprecedented low levels.

In their 2016 work *Universal Smiles*, Hagan et al. extended the SABR framework by introducing an **effective forward equation**, which allows for an asymptotic expansion that applies to a broader class of **stochastic volatility models**, including Heston, mean-reverting SABR, and ZABR-like models. A major result of their analysis is an **explicit asymptotic formula** for **implied normal volatilities** (also known as **Bachelier volatilities**), which are particularly useful for **interest rate options** priced under the **normal model**.

This paper focuses on implementing the **shifted SABR model** for Swaptions, calibrating its parameters to fit the **market physical volatility cube**, and using the derived asymptotic formulas to obtain **normal implied volatilities** efficiently.

1.2 From the SABR Model to Normal Implied Volatilities

1.2.1 The SABR Model and the Effective Forward Equation

The standard **SABR model** describes the evolution of a forward rate $F(T)$ and its stochastic volatility $A(T)$ as follows:

$$dF = \epsilon A\, C(F)\, dW_1, \tag{1}$$

$$dA = \epsilon \nu A \, dW_2, \tag{2}$$

$$dW_1 \, dW_2 = \rho \, dT. \tag{3}$$

where:

- $A(T)$ represents the **volatility process**, assumed to follow a **lognormal process**.
- $C(F) = (F + o)^\beta$ is the **backbone function**, where o accounts for shifts ensuring that $F + o > 0$.
- ρ is the **correlation** between the forward rate and volatility.
- ν is the **volatility of volatility** (vol of vol).
- ϵ is a **small perturbation parameter**.

To obtain **option prices**, one must compute the **marginal density** $Q(T, F)$, which satisfies the Kolmogorov forward equation. However, solving this directly is challenging due to its **two-dimensional nature**. Instead, Hagan et al. propose a **singular perturbation analysis**, reducing the problem to a **one-dimensional effective forward equation**:

$$Q_T = \frac{1}{2}\epsilon^2 \alpha^2 \left(1 + 2\epsilon\rho v z/\alpha + \epsilon^2 v^2 z^2/\alpha^2\right) C^2(F) Q_{FF}. \tag{4}$$

where

$$z = \frac{1}{\epsilon} \int_f^F \frac{dF'}{C(F')}. \tag{5}$$

This equation provides a tractable way to approximate **option prices** under SABR-like models.

1.2.2 Asymptotic Expansion for Normal Implied Volatility

In Appendix A of *Universal Smiles*, Hagan et al. use **singular perturbation techniques** to derive an explicit formula for **implied normal volatility** σ_N, also known as **Bachelier volatility**. This is critical for pricing Swaptions under the **normal model**, which assumes an additive rather than multiplicative structure for price fluctuations.

The asymptotic expansion leads to:

$$\sigma_N(T_{ex}, K) = \epsilon\alpha \cdot \frac{K - f}{\int_f^K \frac{dF}{C(F)}} \cdot \frac{\zeta}{Y(\zeta)} \cdot \begin{cases} 1 + \epsilon^2 \theta(T_{ex}) & \text{if } \theta \geq 0, \\ \frac{1}{1 - \epsilon^2 \theta(T_{ex})} & \text{if } \theta < 0. \end{cases} \tag{6}$$

where:

- $\zeta = \frac{\nu}{\alpha} \int_f^K \frac{dF}{C(F)}$ captures **stochastic volatility effects**.
- $Y(\zeta) = \log\left(\frac{\rho + \zeta + \sqrt{1 + 2\rho\zeta + \zeta^2}}{1 + \rho}\right)$ accounts for **skewness**.

- $\theta(\zeta)$ contains **higher-order corrections**:

$$\theta(\zeta) = \frac{\nu^2}{24}\left(-1 + \frac{3(\rho+\zeta) - \rho E(\zeta)}{Y(\zeta)E(\zeta)}\right) + \frac{\Delta_0\alpha^2}{6}\left(1 - \rho^2 + \frac{(\rho+\zeta)E(\zeta) - \rho}{Y(\zeta)}\right). \tag{7}$$

where:

$$E(\zeta) = \sqrt{1 + 2\rho\zeta + \zeta^2}. \tag{8}$$

The backbone function, usually an **offset CEV function** $C(F) = (F+o)^\beta$, simplifies certain terms:

$$\zeta = \frac{\nu}{\alpha}\frac{(K+o)^{1-\beta} - (f+o)^{1-\beta}}{1-\beta}. \tag{9}$$

$$\Delta_0 = -\frac{1}{8}\beta(2-\beta)(f+o)^{2-2\beta}. \tag{10}$$

1.3 Choice of Implied Normal Volatility Formula for Implementation

The original asymptotic formula for **SABR normal implied volatilities** derived in *Universal Smiles* (Hagan et al., 2016) provides a robust theoretical foundation for pricing and calibration. However, in practical applications, a more numerically stable and computationally efficient version of this formula is often preferred.

In this implementation, we adopt the formulation given by Prof. Bianchetti, which is structurally equivalent to the original but rewritten to facilitate practical calculations. The modified formula for the **SABR normal implied volatility** is:

$$\sigma_N^{SABR}(t;T,\bar{F},\bar{K},p) = \nu(\bar{K}-\bar{F})\frac{Z(z)}{Y(z)}, \tag{11}$$

where the dimensionless parameter z is defined as:

$$z := \frac{\nu}{\bar{\alpha}}\begin{cases}\frac{\bar{K}^{1-\beta} - \bar{F}^{1-\beta}}{1-\beta}, & \text{for } \beta \neq 1,\\ \ln\frac{\bar{K}}{\bar{F}}, & \text{for } \beta = 1.\end{cases} \tag{12}$$

The auxiliary functions involved in the formula are:

$$Y(z) := \ln\frac{z + \rho + E(z)}{1+\rho}, \quad E(z) := \sqrt{1 + 2\rho z + z^2}. \tag{13}$$

The adjustment factor $Z(z)$ accounts for higher-order corrections and is defined as:

$$Z(z) := \begin{cases}1 + \Theta(z)\tau(t,T), & \text{for } \Theta(z) \geq 0,\\ [1 - \Theta(z)\tau(t,T)]^{-1}, & \text{for } \Theta(z) < 0.\end{cases} \tag{14}$$

where the higher-order term $\Theta(z)$ is:

$$\Theta(z) := \frac{\nu^2}{24}\left[-1 + \frac{3z + \rho - \rho E(z)}{Y(z)E(z)}\right] + \frac{\bar{\alpha}^2\Delta_0}{6}\left[1 - \rho^2 + \frac{(z+\rho)E(z) - \rho}{Y(z)}\right]. \quad (15)$$

The correction term Δ_0 is given by:

$$\Delta_0 := \frac{\beta(2-\beta)}{8\bar{F}^{2-2\beta}}. \quad (16)$$

Finally, the **effective volatility parameter** $\bar{\alpha}$ incorporates additional adjustments:

$$\bar{\alpha} := \alpha\left[1 + \frac{1}{4}\alpha\beta\rho\nu\bar{F}^{1-\beta}\tau(t,T)\right]. \quad (17)$$

1.3.1 Relevance to Implementation

Since the task involves implementing the **shifted SABR model** for Swaptions and calibrating it to the **market Swaption volatility cube**, the work focuses on:

- Implementing the **shifted SABR model** dynamics, ensuring the backbone function accounts for negative interest rates.
- Using the derived **normal volatility formula** to compute **implied volatility values** from observed market Swaption prices.
- Calibrating model parameters $(\alpha, \beta, \rho, \nu)$ to fit the **market volatility cube** using least squares optimization.
- Numerically solving the effective forward equation or applying closed-form solutions to obtain option prices and implied volatilities efficiently.

2 Retrieving Market-Implied Normal Volatilities

To calibrate the model parameters, we first need the *market-implied normal volatilities*, which we derive from the Bachelier (normal) pricing formula. In this context, the key inputs are:

- $V(T_{\text{expiry}}, K)$: the *forward* swaption price,
- R^{IRS}: the *forward swap rate*,
- K: the strike of the swaption,
- $\omega = \pm 1$: indicating a payer $(+1)$ or receiver (-1) swaption,
- A_d: the relevant annuity (spot or forward, depending on the exact setup).

2.1 Bachelier (Normal) Pricing Formula

Recalling the Bachelier formula for a payer or receiver swaption with expiry T_{expiry}, forward swap rate R^{IRS}, strike K, and normal volatility σ_N:

$$V_{\text{Bach}}\big(T_{\text{expiry}}, K\big) \;=\; \Big[\omega\,\big(R^{\text{IRS}} - K\big)\,\Phi\big(\omega\,d\big) + \sigma_N\,\sqrt{T_{\text{expiry}}}\,\phi(\omega\,d)\Big], \quad d \;=\; \frac{R^{\text{IRS}} - K}{\sigma_N\,\sqrt{T_{\text{expiry}}}}, \tag{18}$$

where $\omega = +1$ for a *payer* swaption and $\omega = -1$ for a *receiver* swaption. Here, $\Phi(\cdot)$ and $\phi(\cdot)$ denote the standard normal CDF and PDF, respectively.

2.2 Forward Swaption Prices

We obtain the forward swaption price $V(T_{\text{expiry}}, K)$ by taking the *spot* swaption premium (from the Excel file `AIRMM-MarketData31Oct2019`, sheet `Market price cube`, table `EUR Cube Payer/Receiver Swaption Physical Settled Forward Premiums (Eonia discounted)`) and dividing by the *spot annuity*. The spot premia, originally quoted in basis points, are converted into decimal format by dividing by 10,000.

Spot Annuity Calculation. The spot annuity, denoted $A_d(T_e, S)$, is computed as shown below:

$$A_d(T_e, S) \;=\; \sum_{i=1}^{n} P_d\big(T_e; S_i\big)\,\tau_K(S_{i-1}, S_i), \tag{19}$$

where $P_d(T_e; S_i)$ is the OIS discount factor for maturity S_i, and $\tau_K(S_{i-1}, S_i)$ is the year fraction of the fixed leg (annual frequency). To obtain the OIS discount factors P_d, we use data from `AIRMM-MarketData31Oct2019`, sheet `IR yield curve`, table `EUR OIS yield curve`, which contains annualized OIS zero rates. We convert these zero rates into continuously compounded discount factors:

$$P_d(0; T) \;=\; \exp\big(-r_{\text{OIS}}(T)\,T\big),$$

where T is measured in years according to the `ACT/365` convention (days/365). We then apply *monotonic cubic spline* interpolation to obtain discount factors at any intermediate maturities. (See Figure 1 for an of the interpolated OIS discount factor curve.)

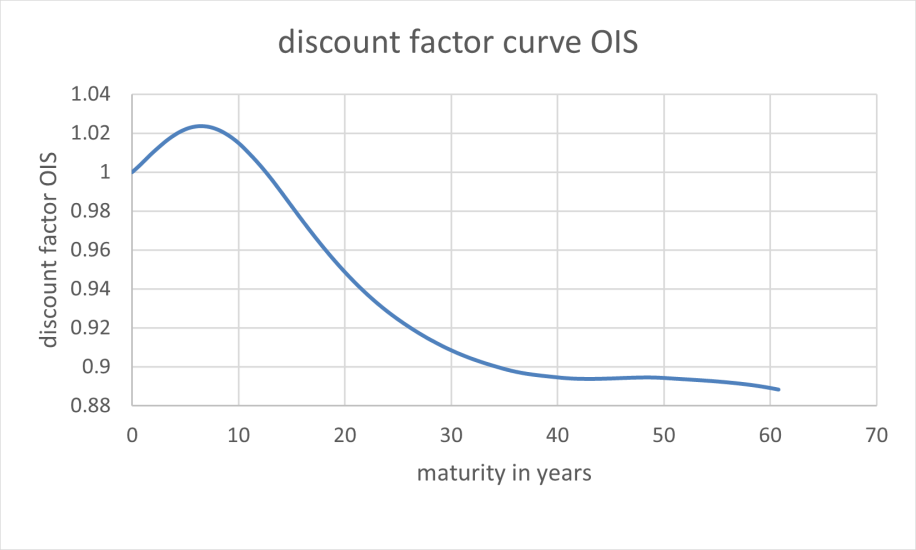

Figure 1: Discount factor curve OIS

2.3 Forward Swap Rate

The second input, R^{IRS}, is the *forward swap rate*. We initially take the forward swap rates from the sheet `IRS 6M forwards` in the same Excel file and convert them from basis points to decimals by dividing by 100. These quoted forward swap rates start from 1 year onward, so short-term maturities are not directly provided. For those missing maturities, we apply the formula shown below:

$$\bar{K} \;:=\; R_x^{\text{IRS}}(t;T,S) \;=\; \frac{\text{IRS}_{\text{float}}(t;T)}{N\,\omega\,A_d\big(t;S\big)} \;=\; \frac{\displaystyle\sum_{j=1}^{m} P_d\big(t;T_j\big)\,F_{x_j}(t)\,\tau_x\big(T_{j-1},T_j\big)}{A_d\big(t;S\big)}. \tag{20}$$

, which essentially requires:

- The OIS discount factor curve $P_d(t;T_i)$,
- The forward IBOR 6M rate $F_{x,i}(t)$,
- The year fraction of the floating leg (semiannual frequency),
- The previously computed spot annuity $A_d(t;S)$.

Forward IBOR 6M Rate. To find $F_{x,i}(t)$ for each relevant payment period, we use the relationship below:

$$F_{x,i}(t) \;=\; \frac{1}{\tau_x(T_{i-1},T_i)}\Big[\frac{P_x(t;T_{i-1})}{P_x(t;T_i)} \;-\; 1\Big], \tag{21}$$

where $P_x(t;T)$ is the discount factor from the *IBOR 6M curve* (again derived from annualized EURIBOR 6M rates in `IR yield curve` via continuously compounded conversion and monotonic spline interpolation). See Figure 2 for an example of the interpolated IBOR discount factor curve. Plugging these forward rates into the second-image formula then yields R^{IRS} for short-term maturities as well.

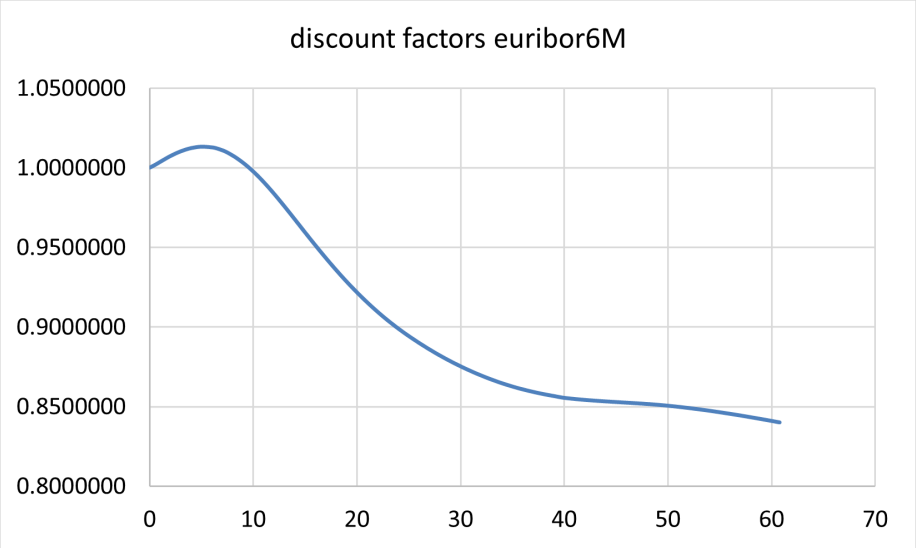

Figure 2: Discount factor curve EURIBOR 6M

2.4 Swaption Strikes

The swaption strikes K come from the same grid used for the spot premia, where they are listed as $\{-400,-200,\ldots,+200,+400\}$ in basis points. We convert them to decimals (dividing by 10,000) and then shift by the forward rate R^{IRS} to get the absolute strike levels:

$$K_{\text{abs}} \;=\; R^{\text{IRS}} \;\pm\; (\text{strike in decimals}).$$

2.5 Bachelier-Implied Volatility Extraction

Finally, to obtain the market-implied *Bachelier normal volatility*, we invert the above Bachelier pricing formula numerically.

Newton–Raphson Root-Finding. We solve for the implied normal volatility σ_N by setting up the difference between the market swaption price V_{mkt} and the Bachelier model price $V_{\text{Bach}}(\sigma_N)$:

$$f(\sigma_N) \;=\; V_{\text{Bach}}(\sigma_N) \;-\; V_{\text{mkt}} \;=\; 0.$$

The Newton–Raphson method iterates

$$\sigma_N^{(n+1)} \;=\; \sigma_N^{(n)} \;-\; \frac{f(\sigma_N^{(n)})}{f'(\sigma_N^{(n)})},$$

where $f'(\sigma_N)$ is the derivative of $f(\sigma_N)$ with respect to σ_N. In practice, we initialize at $\sigma_N^{(0)} = 0.05$ (5%), set a tolerance of 10^{-8}, and allow up to 100 iterations. Once the root is found, we have the *market-implied normal volatility* that matches the observed forward swaption price.
Below there is an example of market implied normal vol, with tenor 10 years. The downward spikes are caused by the value 1e-8 attributed by the Newton-Raphson method when it can't found market quotations inside the swaption premia cube.

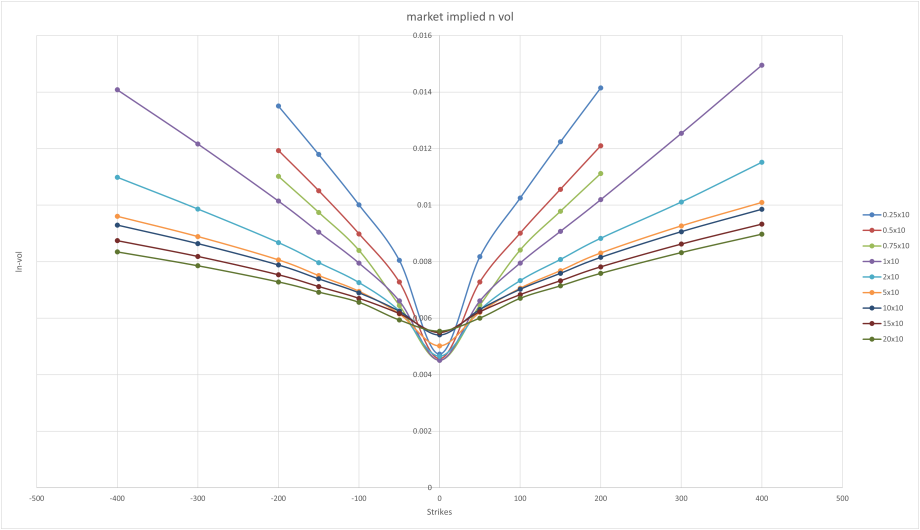

With these implied normal volatilities in hand, we can now proceed to the next stage: calibrating the SABR parameters $(\alpha, \beta, \rho, \nu)$ against the entire grid of swaptions.

Figure 3: Market-implied normal-volatility smile for different expiry and fixed tenor (10 years)

3 Calibration of the Shifted SABR Model

Having retrieved the market-implied Bachelier normal volatilities for a grid of expiries $\{T_{\text{exp}}\}$ and strikes $\{K\}$, we now proceed to calibrate the shifted SABR parameters:

$$\big(\alpha, \beta, \rho, \nu\big).$$

Recall that the shifted SABR model posits the forward process

$$dF_t = \alpha_t \left(F_t + \lambda\right)^{\beta} dW_t^1, \qquad d\alpha_t = \nu\, \alpha_t\, dW_t^2, \qquad \text{corr}(dW^1, dW^2) = \rho,$$

where λ is the shift evaluated to ensure that the forward swap rate is positive.

3.1 Simplified SABR Normal Volatility Formula

For $F \neq K$, we use the simplified asymptotic formula for the SABR normal volatility, which has been reformulated for computational efficiency (11). In the *at-the-money* (ATM) case, i.e., when $F \to K$, we compute the limit of the SABR formula. Specifically, we use:

$$\bar{\alpha} = \alpha \left(1 + 0.25\, \alpha\, \beta\, \rho\, \nu\, (F_b)^{1-\beta}\, \frac{T}{365}\right), \tag{22}$$

$$\sigma_{N,\text{ATM}} \approx \bar{\alpha}\, (F_b)^{\beta} \left(1 + \frac{\nu^2}{24}\, \frac{\bar{\alpha}^2}{(F_b)^{2\beta}} + \frac{\rho\, \nu\, \bar{\alpha}}{4\, (F_b)^{\beta}}\right), \tag{23}$$

where F_b denotes the forward swap rate for the ATM swaption and T is the time to expiry in days.

For $F \neq K$, the simplified SABR normal volatility formula is applied directly.

3.2 Objective Function and Minimization

To calibrate $(\alpha, \beta, \rho, \nu)$, we minimize the root-mean-square error (RMSE) between the model-implied normal volatilities σ_N^{SABR} and the market-implied normal volatilities σ_N^{mkt}:

$$\text{RMSE}\big(\alpha, \beta, \rho, \nu\big) \;=\; \sqrt{\frac{1}{N} \sum_{T_{\text{exp}}} \sum_{K} \Big[\sigma_N^{\text{SABR}}\big(T_{\text{exp}}, K;\, \alpha, \beta, \rho, \nu\big) \;-\; \sigma_N^{\text{mkt}}\big(T_{\text{exp}}, K\big)\Big]^2}, \tag{24}$$

where N is the total number of calibration points.

We use the L-BFGS-B optimization algorithm to minimize this RMSE. The initial guesses for the parameters were set as:

$$\alpha_0 = 0.02, \quad \beta_0 = 0.5, \quad \rho_0 = -0.5, \quad \nu_0 = 0.3.$$

3.3 Calibration Procedure

1. **Initialization.** Start with the initial parameter guesses:

$$(\alpha, \beta, \rho, \nu) = (0.02,\ 0.5,\ -0.5,\ 0.3).$$

2. **Model-Implied Normal Volatility.** For each calibration point (T_{exp}, K), compute the SABR normal implied volatility using the simplified formula for $F \neq K$ (11) and the ATM limit given by Equations (22) and (23) for the ATM case.

3. **Objective Evaluation.** Evaluate the RMSE as in Equation (24).

4. **Optimization.** Use the L-BFGS-B algorithm to adjust the parameters and minimize the RMSE. The L-BFGS-B algorithm is a variant of the Broyden–Fletcher–Goldfarb–Shanno (BFGS) quasi-Newton method designed to handle bound constraints on parameters. Its key features include:

   - **Limited Memory Usage:** Instead of storing the full Hessian matrix, L-BFGS-B approximates its inverse using a limited set of vectors, making it particularly efficient for problems with a moderate to large number of parameters.
   - **Bound Constraints:** The algorithm naturally incorporates lower and upper bounds for each parameter. This is crucial for our calibration, as it allows us to enforce realistic limits (e.g., $\beta \in [0, 1]$, $\rho \in [-1, 1]$, and ensuring $\alpha, \nu > 0$).
   - **Rapid Convergence:** By leveraging gradient information to approximate second-order behavior of the objective function, L-BFGS-B often converges faster than simple gradient descent methods.

5. **Convergence.** Check for convergence. If not converged, iterate until the stopping criteria are met.

Upon convergence, the calibrated parameters $(\alpha^*, \beta^*, \rho^*, \nu^*)$ are obtained. Below there is a graph representing the volatility smile for tenor = 10y.

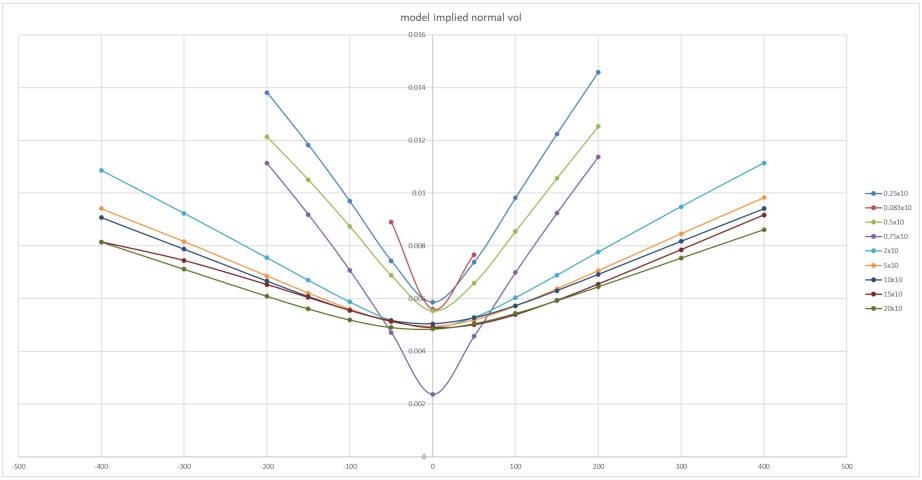

Figure 4: Model-implied normal-volatility smile for different expiry and fixed tenor (10 years)

4 Comparison of Different Objective Functions

To assess the *calibration precision* of the shifted SABR model, we tested several objective functions:

- **Relative price differences:** minimize $\sum \left(\frac{V_{\text{model}} - V_{\text{market}}}{V_{\text{market}}} \right)^2$, where V_{model} and V_{market} are the model and market swaption prices, respectively.
- **RMSE of volatility:** minimize $\sqrt{\frac{1}{N} \sum \left(\sigma_{N,\text{model}} - \sigma_{N,\text{market}} \right)^2}$, where $\sigma_{N,\text{model}}$ and $\sigma_{N,\text{market}}$ are the model and market Bachelier-implied volatilities.
- **Vega-weighted RMSE of volatility:** similar to the volatility RMSE, but each squared difference is multiplied by a weight proportional to the option's *vega*, giving more importance to at-the-money points (where vega is typically higher).

4.1 Interpretation of Calibration Errors for Different Expiries (Fixed Tenor)

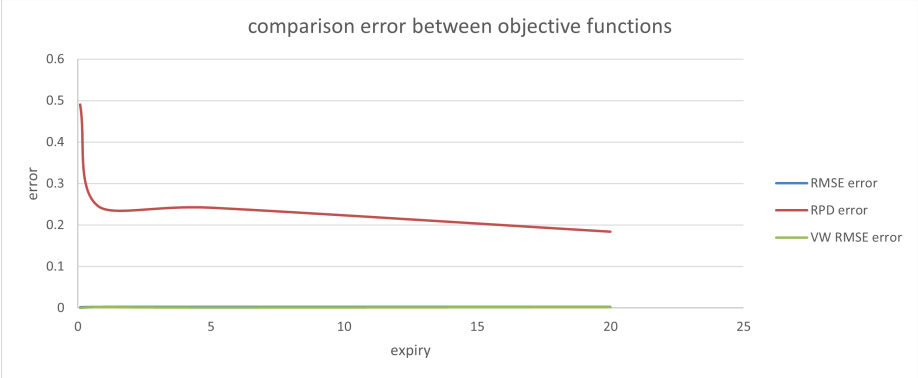

Figure 5: Comparison between errors between different objective functions: Relative Price Difference, Root Mean Square Error, Vega Weighted Root Mean Square Error

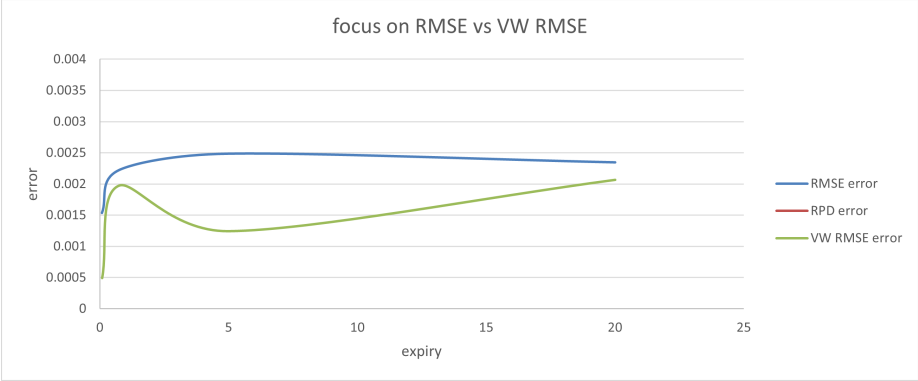

Figure 6: Focus on the error difference between RMSE and VW RMSE

Figures **??** and **??** illustrate how the calibration error behaves as a function of the *expiry* for a fixed tenor (5 years). Three objective functions are compared:

- **RPD** (*Relative Price Difference*),
- **RMSE** (*Root Mean Square Error* of implied vol),
- **VW RMSE** (*Vega-Weighted* RMSE of implied vol).

First Chart (All Three Errors) In Figure **??**, the vertical axis shows the error, while the horizontal axis is the expiry. We see that:

- The **RPD error** (red line) starts off relatively large at short expiries, then declines and eventually flattens out. This is expected, as relative price differences can become more pronounced when the absolute swaption price is small (often the case for short maturities).
- Both **RMSE** (blue) and **VW RMSE** (green) lie well below the RPD curve on this scale. Between the two volatility-based metrics, RMSE is slightly higher than VW RMSE over much of the expiry range.

Second Chart (Focused Scale on RMSE vs. VW RMSE) In Figure **??**, we zoom in to compare only **RMSE** (blue) and **VW RMSE** (green). The RPD error is excluded here because it is larger and would dominate the scale. We observe:

- The two curves are close, but the VW RMSE generally remains below the standard RMSE for shorter and medium expiries.
- As expiry increases, the two lines converge, indicating that for long maturities, the distinction between simple RMSE and vega-weighted RMSE becomes less pronounced in this dataset.

Overall, these plots show that **RPD** behaves quite differently from the volatility-based errors, especially for short expiries, while **VW RMSE** consistently yields a slightly lower error than standard RMSE. However, at longer expiries, the two volatility-based metrics become nearly indistinguishable.

5 Comparison of Optimization Algorithms: Precision vs. Performance

This section compares four different optimization algorithms—`L-BFGS-B`, `Nelder-Mead`, `Powell`, and `CMA-ES`—used to calibrate the shifted SABR model across various expiries (from 0.0833 years to 20 years) for a fixed tenor of 5 years. Table **??** summarizes the results, including the calibrated parameters $(\alpha, \beta, \rho, \nu)$, the calibration error (RMSE), the number of iterations, runtime, and whether the method converged.

5.1 Brief Overview of the Four Algorithms

L-BFGS-B

- **Algorithm Type:** Quasi-Newton, gradient-based.
- **Key Feature:** Maintains a limited-memory approximation of the inverse Hessian, allowing it to handle moderate to large dimensions efficiently.

- **Bound Constraints:** Naturally accommodates parameter bounds, which is useful for restricting $(\alpha, \beta, \rho, \nu)$ to realistic domains.
- **Pros:**
  - Converges quickly when a decent initial guess is available.
  - Efficient in terms of memory and runtime.
- **Cons:**
  - A local method, so it can get trapped in local minima if the surface is highly non-convex.
  - Requires gradient information or approximations (finite differences), which can be sensitive to step-size choices.

Nelder-Mead

- **Algorithm Type:** Direct search (simplex) method, derivative-free.
- **Key Feature:** Explores the parameter space by expanding and contracting a simplex based on function values at the vertices.
- **Pros:**
  - No gradient needed, which can simplify coding for complicated objective functions.
  - Often works well in lower-dimensional spaces with smooth, unimodal surfaces.
- **Cons:**
  - May fail to converge on complicated or ill-conditioned surfaces.
  - Typically slower (more iterations) than gradient-based approaches.
  - No native mechanism for bound constraints (though variants exist).

Powell

- **Algorithm Type:** Derivative-free line search.
- **Key Feature:** Successively refines a set of directions and does 1D minimizations along each direction.
- **Pros:**
  - No gradients required.
  - Straightforward to implement for moderate-dimensional, well-behaved functions.
- **Cons:**

  - Can stall or fail if the surface has narrow valleys or is highly non-linear.
  - Not designed to handle parameter bounds by default.

CMA-ES (Covariance Matrix Adaptation Evolution Strategy)

- **Algorithm Type:** Evolutionary, population-based.
- **Key Feature:** Maintains a population of candidate solutions, adapting a multivariate Gaussian to explore the space globally.
- **Pros:**
  - Strong global search capabilities; less prone to local minima.
  - Does not require gradients, suitable for non-smooth or noisy objectives.
- **Cons:**
  - Generally requires more function evaluations (slower in CPU time) than gradient-based methods.
  - Has several hyperparameters (e.g., population size, stopping criteria) that may need tuning.

5.2 Empirical Results and Observations

Table **??** presents the calibration outcomes for each method at different expiries:

- **L-BFGS-B** consistently converges with low errors ($\approx$ 0.0014–0.0025 in RMSE) and modest iteration counts. Its runtime is also relatively short, making it both *fast* and *accurate* when starting from a decent initial guess.
- **Nelder-Mead** converges successfully for some expiries (e.g., 0.0833y, 5y) but fails for others (0.75y, 20y). Where it does converge, it yields errors comparable to L-BFGS-B, but at the cost of more iterations (e.g., 326 vs. 40). This suggests that Nelder-Mead is more sensitive to local minima or surface topology in the SABR calibration.
- **Powell** does not converge for any of the tested expiries in our dataset. This could reflect the complexity of the SABR objective surface, especially given no gradient or bound constraints are inherently applied in the basic Powell method.
- **CMA-ES** converges in all tested scenarios, achieving errors similar to L-BFGS-B. However, it often requires substantially more iterations (up to 595) and longer CPU time (e.g., $\sim$ 1.7 seconds vs. $<$ 0.1 seconds for L-BFGS-B). This aligns with CMA-ES's reputation as a robust global method that trades speed for thorough exploration.

Overall Comparison.

- **L-BFGS-B** emerges as the most efficient method for this calibration problem, given suitable initial guesses and the ability to compute or approximate gradients.
- **CMA-ES** offers a stronger global search, which can be valuable if local minima are suspected, but at a higher computational cost.
- **Nelder-Mead** and **Powell** are both gradient-free, but in practice they are more prone to stalling or failing in this SABR context, particularly for certain expiries where the objective surface appears to be more complex.

In summary, if the goal is *speed and reliability* for typical SABR calibration tasks, **L-BFGS-B** is recommended. If one needs a more global approach, **CMA-ES** is a good fallback, albeit slower. For non-smooth or black-box objective functions where gradients are unavailable, direct search methods like **Nelder-Mead** or **Powell** may be tried, but with caution regarding potential convergence issues.

expiry	ward swap	method	alpha	beta	rho	nu	rror (RMSE	iterations	time (s)	converged
0.083333	-0.00256	L-BFGS-B	0.074348	1	0.98	0.577551	0.001447	40	0.015876	TRUE
0.75	-0.00203	L-BFGS-B	0.164068	1	0.257643	0.520568	0.002043	36	0.021186	TRUE
5	0.0031	L-BFGS-B	0.014638	0.245172	-0.89001	0.582791	0.002488	31	0.027573	TRUE
20	0.00603	L-BFGS-B	0.00904	0	0.235354	0.721003	0.002349	61	0.064569	TRUE
0.083333	-0.00256	Nelder-Me	0.254079	1.526228	7.255186	0.030008	1.36E-08	326	0.012783	TRUE
0.75	-0.00203	Nelder-Mead							0.03801	FALSE
5	0.0031	Nelder-Me	0.014624	0.24488	-0.88998	0.582801	0.002488	187	0.01731	TRUE
20	0.00603	Nelder-Mead							0.043758	FALSE
0.083333	-0.00256	Powell							0.001055	FALSE
0.75	-0.00203	Powell							0.001784	FALSE
5	0.0031	Powell							0.002527	FALSE
20	0.00603	Powell							0.002184	FALSE
0.083333	-0.00256	CMA-ES	0.074349	1	0.98	0.577592	0.001446	595	1.773772	{'tolstagnation': 198}
0.75	-0.00203	CMA-ES	0.164067	1	0.257573	0.520456	0.002042	535	1.794535	{'tolstagnation': 198}
5	0.0031	CMA-ES	0.014624	0.244881	-0.88998	0.582799	0.002488	147	0.498398	{'tolfun': 1e-11}
20	0.00603	CMA-ES	0.00904	6.92E-12	0.235346	0.720995	0.002349	235	0.79125	{'tolfun': 1e-11}

Figure 7: Comparison between different optimisation algorithms: L-BFGS-B, Nelder-Mead, Powell, CMA-ES

6 SABR Parameter Redundancy Analysis

A known challenge in SABR calibration is the potential *redundancy* among its parameters. In other words, different combinations of α, β, ν, and ρ can produce very similar implied volatility smiles, making it difficult to pin down unique parameter values. To explore this, we vary one parameter at a time (fixing it at different levels) while allowing the other parameters to adjust. The resulting normal implied volatilities are plotted in Figures **??**–**??**.

Varying α. In Figure **??**, α takes values $\{0.01, 0.02, 0.03, 0.04\}$. The four curves nearly overlap, indicating that adjusting α can be largely compensated by corresponding changes in β, ν, and ρ. Hence, α exhibits a high degree of redundancy: different α-levels still produce very similar smiles once the other parameters are re-optimized.

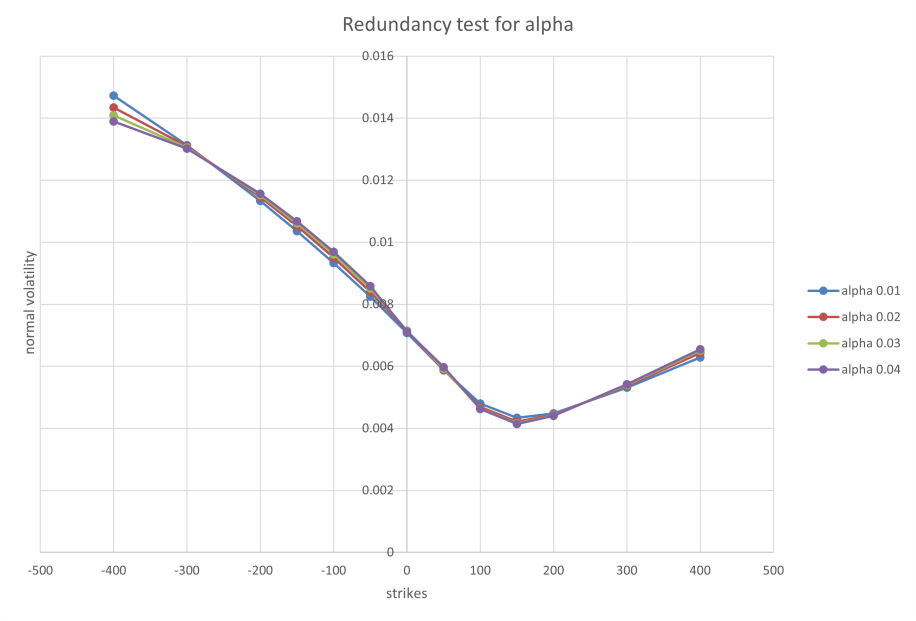

Figure 8: Redundancy test of alpha

Varying β. Figure **??** shows $\beta \in \{0, 0.25, 0.5, 0.75\}$. Again, the implied volatility curves lie close together, indicating that β can also be "traded off" with the remaining parameters. Although there is a slight separation in the wings, the overall shapes remain quite similar, demonstrating that β has partial redundancy in determining the final smile.

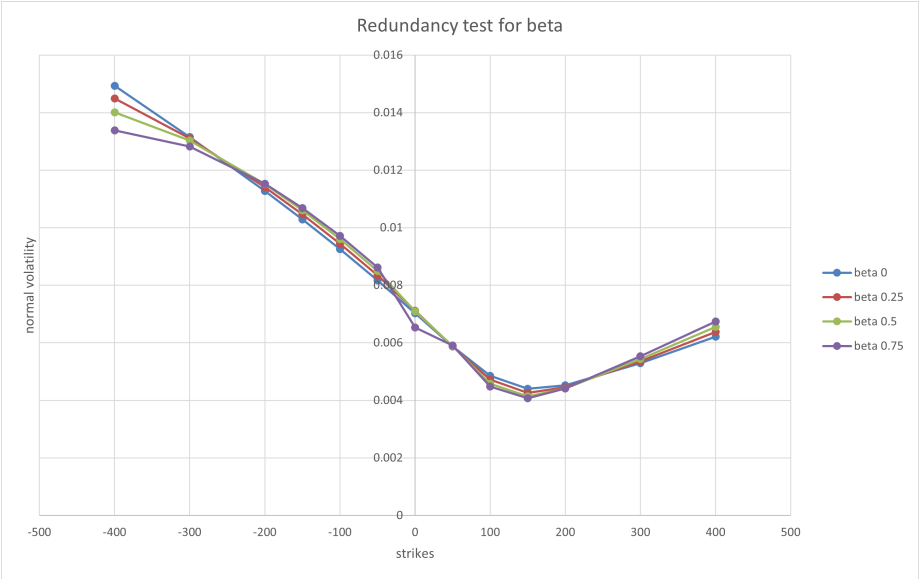

Figure 9: Redundancy test of beta

Varying ν. By contrast, in Figure **??** where ν takes values $\{0.1, 0.2, 0.3, 0.4\}$, we see more pronounced differences across strikes—especially in the wings. This suggests that ν (the "vol-of-vol") exerts a stronger influence on the curvature of the smile, making it less interchangeable with other parameters. Thus, adjusting ν alone does not always yield the same final shape, even if α, β, and ρ are recalibrated.

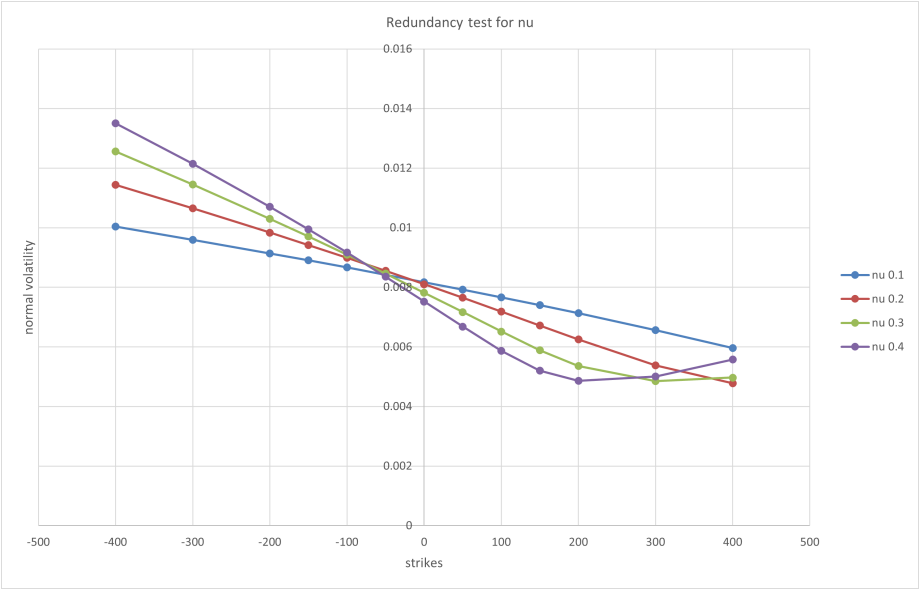

Figure 10: Redundancy test of nu

Varying ρ. Finally, Figure **??** plots $\rho \in \{-0.99, -0.5, 0, 0.5\}$. Here, the shape differences are quite large: negative correlation ($\rho < 0$) drives a significant skew on the left side, whereas positive ρ skews the smile in the opposite direction. No simple adjustments of α, β, and ν can replicate such distinctly different skews. Hence, ρ shows even less redundancy than ν.

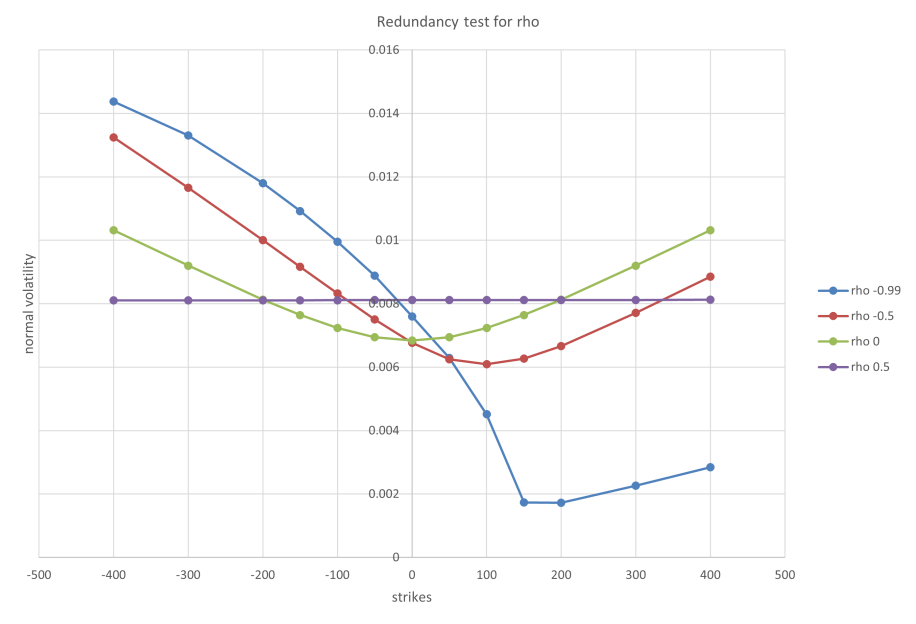

Figure 11: Redundancy test of rho

Conclusions. From these "redundancy tests," we observe:

- α and β exhibit *high redundancy*, meaning that large changes in these parameters can often be offset by recalibrating the other parameters, resulting in similar implied volatility curves.
- ν and ρ, on the other hand, are *less redundant*, since variations in these parameters produce more distinctive changes in the smile shape (particularly in the wings and skew).

This underscores why practical SABR calibrations often fix β *a priori* or place tight bounds on ρ, to reduce degeneracy and achieve more stable calibration results.

7 Computation of Normal and Shifted Lognormal Implied Volatilities

We aim to compute two sets of market-implied volatilities for each swaption:

- σ_N: the *normal* (Bachelier) implied volatility,

- σ_{SLN}: the *shifted lognormal* implied volatility, using a shift λ to ensure $F + \lambda > 0$.

The normal implied volatilities σ_N are already available from Section 2. We now focus on deriving σ_{SLN} by inverting the shifted-Black formula.

7.1 Shifted Lognormal Implied Volatility

Recall the shifted-Black formula for a European call (or payer swaption) payoff, where the forward rate is F and the shift is λ. The premium $V_{\text{shifted-Black}}$ can be written as

$$V_{\text{shifted-Black}}\big(F, K, \sigma_{SLN}\big) \;=\; A_d\left[(F+\lambda)\,\Phi(d_1) \;-\; (K+\lambda)\,\Phi(d_2)\right], \qquad (25)$$

where

$$d_1 \;=\; \frac{\ln\!\big(\frac{F+\lambda}{K+\lambda}\big)}{\sigma_{SLN}\sqrt{T}} + \frac{\sigma_{SLN}\sqrt{T}}{2}, \quad d_2 \;=\; d_1 \;-\; \sigma_{SLN}\sqrt{T},$$

Φ is the standard normal CDF, T is the time to expiry, and A_d is the appropriate annuity or discounting factor. Given a market swaption price V_{mkt}, we *invert* this formula to find σ_{SLN}.

7.2 Brent's Method for Root-Finding

Initially, we attempted to use the *Newton–Raphson* method to solve

$$f\big(\sigma_{SLN}\big) \;=\; V_{\text{shifted-Black}}\big(\sigma_{SLN}\big) \;-\; V_{\text{mkt}} \;=\; 0,$$

but encountered numerical issues whenever $\frac{\partial f}{\partial \sigma_{SLN}}$ became very small (e.g. near deep ITM or OTM points).

Instead, we switched to **Brent's method**, a robust *hybrid* root-finding algorithm that combines:

- **Bisection**, which guarantees convergence if the sign of f changes over an interval,
- **Secant** and **Inverse Quadratic Interpolation**, which can accelerate convergence when the function is well-behaved.

Brent's method does not rely on evaluating derivatives, making it more stable in scenarios where the gradient is small or discontinuous. The general steps are:

1. Identify an interval $[a, b]$ such that $f(a)$ and $f(b)$ have opposite signs.
2. Use a combination of bisection and interpolation to narrow the bracket until σ_{SLN} is found within a chosen tolerance (tolerance chosen = 10^{-8}, max iteration = 1000).

The interval chosen is: lower bound=1e-8, upper bound=5.0.

7.3 Plotting the Market-Implied Normal Volatilities

To visualize the *normal* implied volatilities σ_N across different strikes (or moneyness) and expiries, we can generate a 2D chart. For example, in LaTeX using `pgfplots`:

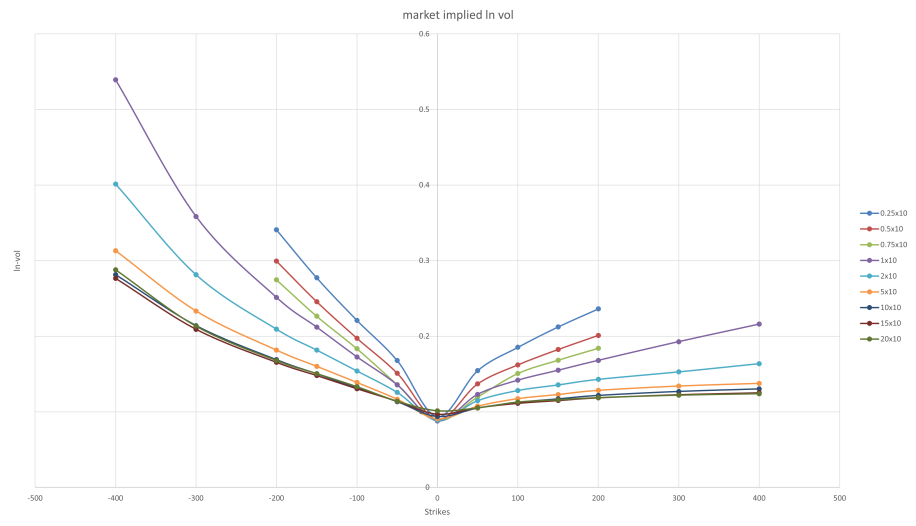

Figure 12: Market-implied normal volatilities σ_N for various strikes and expiries.

8 Approximating Shifted Lognormal Volatilities from Normal Volatilities

In practice, market participants often quote *normal* (Bachelier) implied volatilities, yet certain pricing or risk-management tasks require *shifted lognormal* implied volatilities. To bridge this gap, we can apply an approximate analytic transformation that converts a normal implied volatility, σ_N, into a shifted lognormal volatility, σ'_{SLN}.

8.1 Approximation Formula

Following a simplified version of Hagan et al. ("Universal Smiles"), the shifted lognormal volatility σ'_{SLN} can be approximated as:

$$\sigma'_{\text{SLN}}\big(F, K, \sigma_N\big) \;\approx\; \sigma_N \;\times\; \frac{\ln\!\left(\frac{F+\lambda}{K+\lambda}\right)}{F-K} \;\times\; \Big(1 + \text{small correction terms}\Big),$$

where F is the forward swap rate, K is the strike, and $\lambda > 0$ is the shift ensuring $F + \lambda > 0$. The *correction terms* typically depend on the ATM normal volatility, the time-to-expiry, and the shifted forwards $(F + \lambda)$ and $(K + \lambda)$.

ATM Limit. When $F \approx K$, the expression $\ln\left(\frac{F+\lambda}{K+\lambda}\right)/(F - K)$ becomes numerically unstable. A common workaround is to take the limit:

$$\lim_{K \to F} \frac{\ln\left(\frac{F+\lambda}{K+\lambda}\right)}{F - K} = \frac{1}{F + \lambda}.$$

Hence, near ATM, one replaces the log-term by $1/(F + \lambda)$.

8.2 Implementation and Data Flow

To apply this approximation:

1. **Identify the relevant data** for each swaption: the forward swap rate F, the strike K, the shifted forward and strike $(F + \lambda)$, $(K + \lambda)$, and the normal implied vol σ_N.
2. **Extract the ATM normal vol** $\sigma_{N,\text{ATM}}$ for the same expiry and tenor, used in the correction factor (e.g., $\left[1 + \frac{\sigma_{N,\text{ATM}}^2 T}{24(F+\lambda)(K+\lambda)}\right]$).
3. **Handle the ATM case** separately if $F - K$ is small, using the limit formula $\sigma_N/(F + \lambda)$.
4. **Compute the shifted lognormal vol** σ'_{SLN} via the approximate transformation.

8.3 Plotting the Approximate Shifted LN Volatilities

After computing the shifted lognormal vols, it is helpful to visualize the resulting surface or smile. For instance, you might create a 2D plot of σ'_{SLN} versus the strike (for fixed expiry) or a 3D surface if multiple expiries are available. In LaTeX, one can use `pgfplots`:

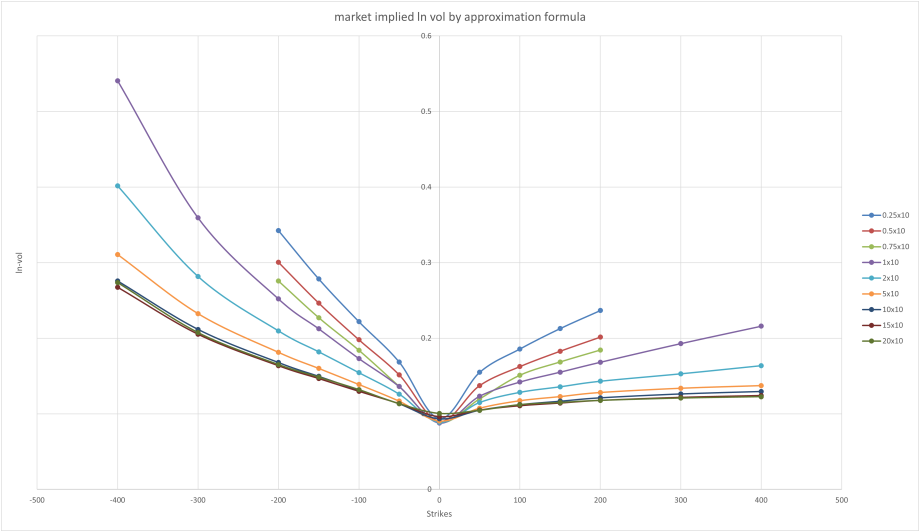

Figure 13: Market implied lognormal volatility smile using as market-vols the ones obtained with the approximation formula

8.4 SABR Calibration Using the Shifted-Lognormal Formula

Before generating the comparison plots, we *calibrated the SABR model* to two different sets of market implied volatilities using the **shifted-lognormal** version of the SABR formula. For non-ATM options ($F \neq K$), Obłój (2008) give the implied lognormal volatility as

$$\sigma_{LN}^{\text{SABR}}(t;T,F,K,p) \;=\; \frac{\nu\,\ln\!\left(\frac{\bar{F}}{\bar{K}}\right)}{Y(z)}\,\Big[1+\ldots\Big], \quad \text{where} \quad z \;=\; \frac{\nu}{\alpha}\,(\bar{F}\bar{K})^{\frac{1-\beta}{2}}\,\ln\!\left(\frac{\bar{F}}{\bar{K}}\right),$$

$\bar{F} = F + \lambda$, $\bar{K} = K + \lambda$ (the shifted forward and strike), and $Y(z)$ is a function of z and the correlation ρ. In the *ATM case* ($F = K$), the usual expansion (see Obłój, 2008) simplifies to

$$\sigma_{LN}^{\text{SABR}}(t;T,F,\text{ATM}) \;=\; \frac{\alpha}{(F+\lambda)^{\,1-\beta}}\left(1 \;+\; \frac{\alpha^2\,(1-\beta)^2}{24\,(F+\lambda)^{\,2-2\beta}} \;+\; \frac{\alpha\,\beta\,\rho\,\nu}{4\,(F+\lambda)^{\,1-\beta}} \;+\; \frac{(2-3\rho^2)\,\nu^2}{24}\right)\tau(t,T) + \ldots$$

Here, α, β, ρ, ν are the usual SABR parameters, and λ is a positive shift ensuring $F + \lambda > 0$. By *inverting* this shifted-Black formula (either numerically or via expansions), we obtain $\sigma_{LN}^{\text{SABR}}$ that matches the given market data. We repeated this calibration process separately for each set of implied volatilities, yielding two different parameter sets. In the following section, we show how these two calibrated lognormal surfaces compare by plotting their differences across various strikes and expiries.

9 Comparison of σ_{SLN} vs. σ'_{SLN}

We conclude our analysis by comparing two sets of shifted lognormal model-implied volatilities:

- σ_{SLN}: obtained via a more precise (e.g. Brent-based) numerical inversion of the shifted-Black formula,
- σ'_{SLN}: derived from an approximate approach.

We investigate how the *difference* between these two vol surfaces,

$$\Delta\sigma_{\text{SLN}}(K,T) \;=\; \sigma_{SLN}(K,T) \;-\; \sigma'_{SLN}(K,T),$$

varies across *moneyness* (ITM, ATM, OTM), expiry, and the SABR parameters α, β, ρ, ν, and shift λ.

9.1 Setup and Plots

We fix a tenor of 5 years and examine three expiries: $\{0.5,\ 5,\ 20\}$ years. For each expiry, we define a grid of relative moneyness $(K-F)$ from -0.05 to $+0.05$. We then vary each SABR parameter in turn, holding the others at baseline values, to see how $\Delta\sigma_{\text{SLN}}$ changes. The code splits the domain into three regions:

- *In-the-money (ITM):* $K - F < -0.0167$,
- *At-the-money (ATM):* $K - F \leq 0.0167$,
- *Out-of-the-money (OTM):* $K - F > 0.0167$.

Figures **??**–**??** display the difference $\left(\sigma_{SLN} - \sigma'_{SLN}\right)$ versus relative moneyness, for each parameter grid and region.

9.2 Observations by Parameter

Varying α. As seen in Figures showing $\Delta\sigma_{\text{SLN}}$ for $\alpha \in \{0.01, 0.02, 0.03\}$, the difference remains relatively small near the ATM region. In the ITM and OTM wings, however, higher values of α (which broadly scales the overall volatility level) can amplify the discrepancy, especially for short expiries (e.g. $T = 0.5$) where the model is most sensitive to the absolute vol level. Overall, α shifts the smile up or down, and if the approximate approach is calibrated with a slightly different α than the Brent-based approach, the mismatch is most pronounced away from ATM.

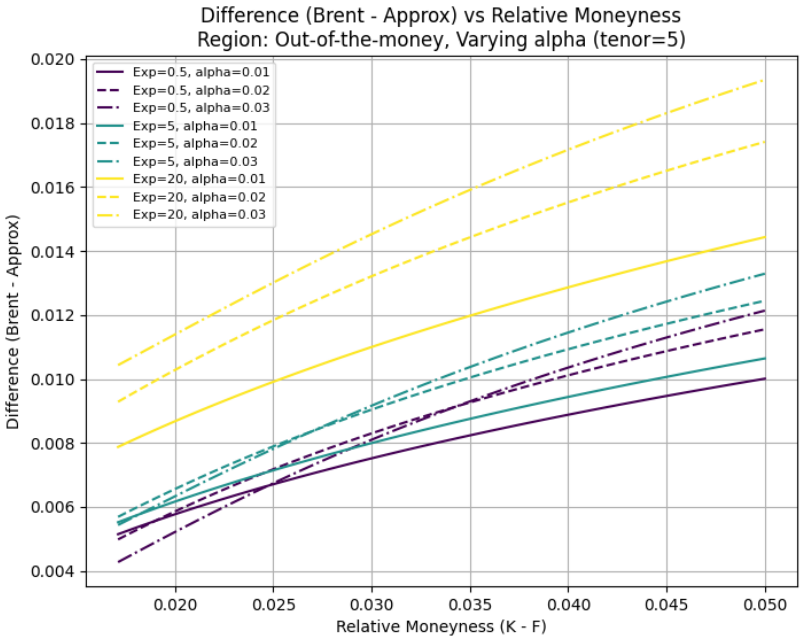
Difference (Brent - Approx) vs Relative Moneyness
Region: Out-of-the-money, Varying alpha (tenor=5)
Exp=0.5, alpha=0.01
Exp=0.5, alpha=0.02
Exp=0.5, alpha=0.03
Exp=5, alpha=0.01
Exp=5, alpha=0.02
Exp=5, alpha=0.03
Exp=20, alpha=0.01
Exp=20, alpha=0.02
Exp=20, alpha=0.03
Difference (Brent - Approx)
Relative Moneyness (K - F)
0.020
0.018
0.016
0.014
0.012
0.010
0.008
0.006
0.004
0.020
0.025
0.030
0.035
0.040
0.045
0.050

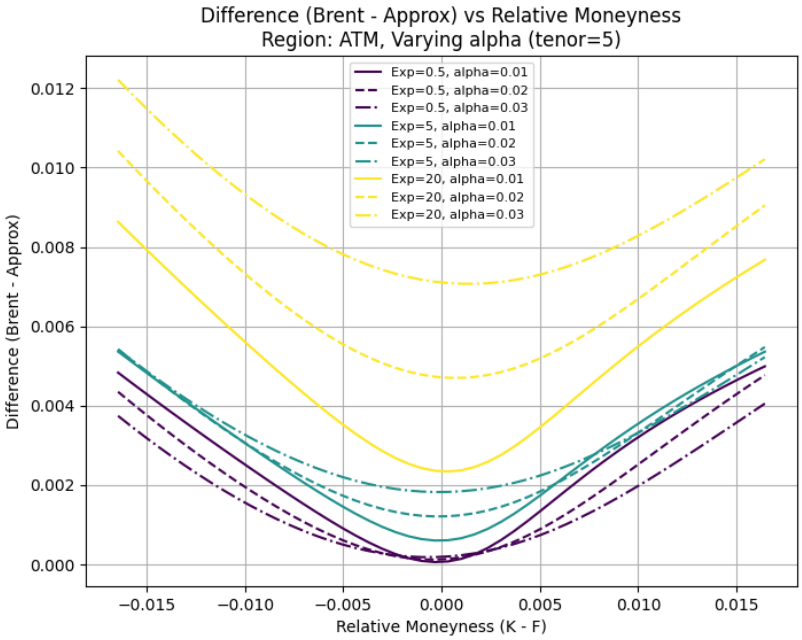
Difference (Brent - Approx) vs Relative Moneyness
Region: ATM, Varying alpha (tenor=5)
Exp=0.5, alpha=0.01
Exp=0.5, alpha=0.02
Exp=0.5, alpha=0.03
Exp=5, alpha=0.01
Exp=5, alpha=0.02
Exp=5, alpha=0.03
Exp=20, alpha=0.01
Exp=20, alpha=0.02
Exp=20, alpha=0.03
Difference (Brent - Approx)
Relative Moneyness (K - F)
0.012
0.010
0.008
0.006
0.004
0.002
0.000
−0.015
−0.010
−0.005
0.000
0.005
0.010
0.015

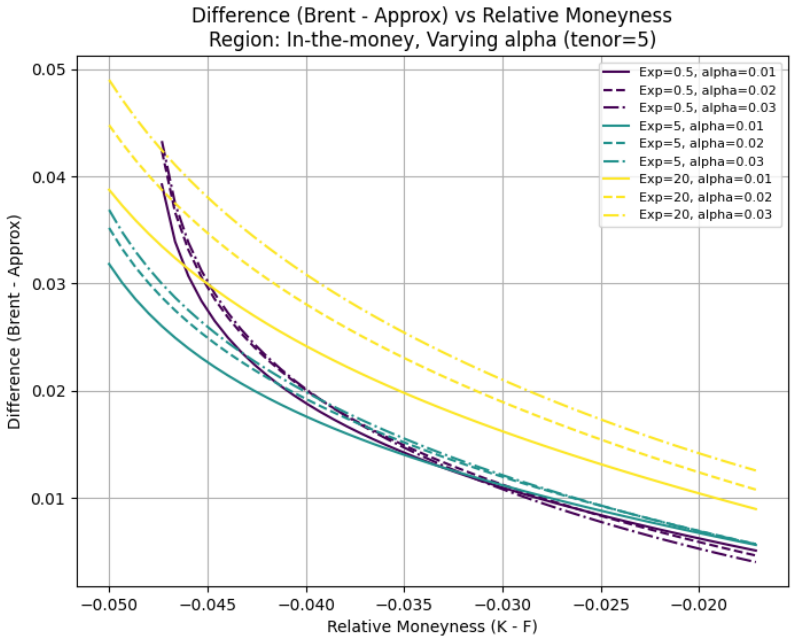

Varying β. For $\beta \in \{0.4, 0.5, 0.6\}$, the difference plots reveal that higher β values often increase $\Delta\sigma_{\text{SLN}}$, particularly in the ITM region. Since β controls the curvature dependence on the forward level, changes in β have a more noticeable effect in the wings. The ATM region is again less sensitive, showing comparatively smaller differences. We also observe that longer expiries (e.g. $T = 20$) can exhibit systematically larger offsets for certain β values, reflecting how the model extrapolates into higher maturities.

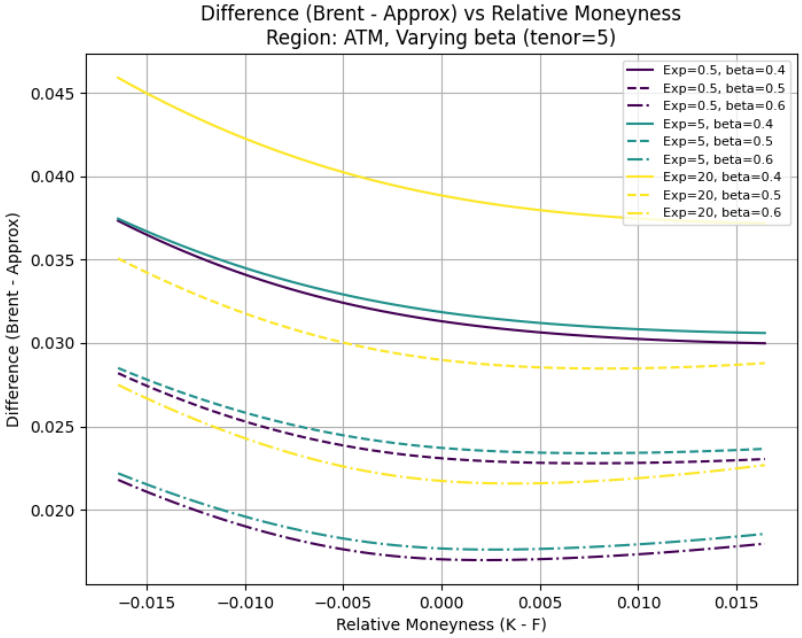
Difference (Brent - Approx) vs Relative Moneyness
Region: ATM, Varying beta (tenor=5)
Exp=0.5, beta=0.4
Exp=0.5, beta=0.5
Exp=0.5, beta=0.6
Exp=5, beta=0.4
Exp=5, beta=0.5
Exp=5, beta=0.6
Exp=20, beta=0.4
Exp=20, beta=0.5
Exp=20, beta=0.6
Difference (Brent - Approx)
0.045
0.040
0.035
0.030
0.025
0.020
−0.015
−0.010
−0.005
0.000
0.005
0.010
0.015
Relative Moneyness (K - F)

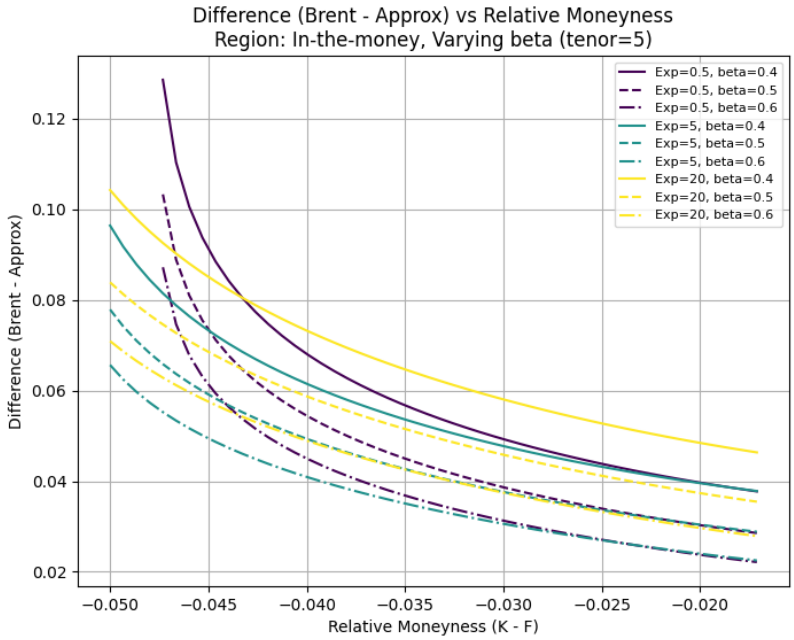
Difference (Brent - Approx) vs Relative Moneyness
Region: In-the-money, Varying beta (tenor=5)
Exp=0.5, beta=0.4
Exp=0.5, beta=0.5
Exp=0.5, beta=0.6
Exp=5, beta=0.4
Exp=5, beta=0.5
Exp=5, beta=0.6
Exp=20, beta=0.4
Exp=20, beta=0.5
Exp=20, beta=0.6
Difference (Brent - Approx)
0.12
0.10
0.08
0.06
0.04
0.02
−0.050
−0.045
−0.040
−0.035
−0.030
−0.025
−0.020
Relative Moneyness (K - F)

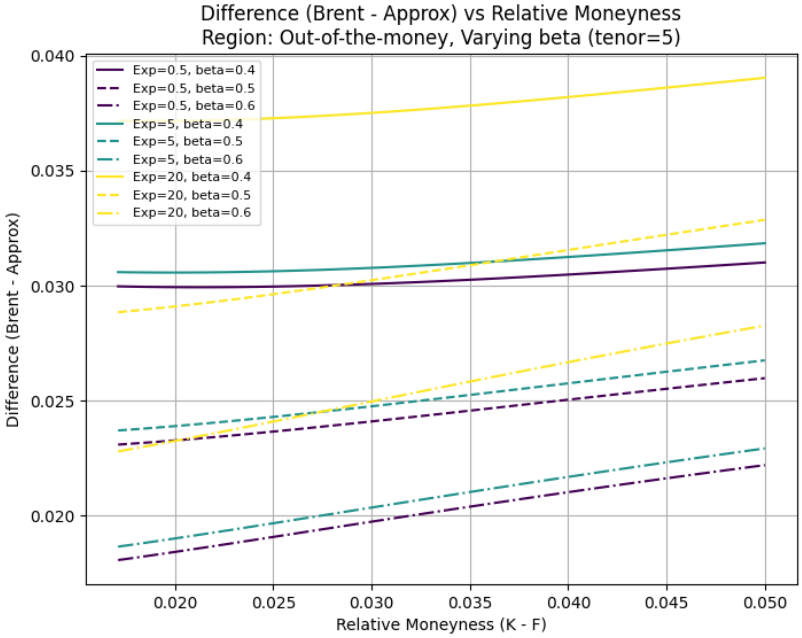

Varying ν. The parameter ν (vol-of-vol) strongly influences the shape and skew of the implied volatility smile. From the plots with $\nu \in \{0.2, 0.3, 0.4\}$, we see that the difference curves can change more significantly across the entire moneyness range. In particular, higher ν often leads to a larger mismatch in the far wings, since vol-of-vol amplifies curvature and skew. The ATM region remains comparatively stable, but ITM and OTM differences can reach higher levels, especially for short maturities where high vol-of-vol can cause the local model expansions to diverge more from the approximate approach.

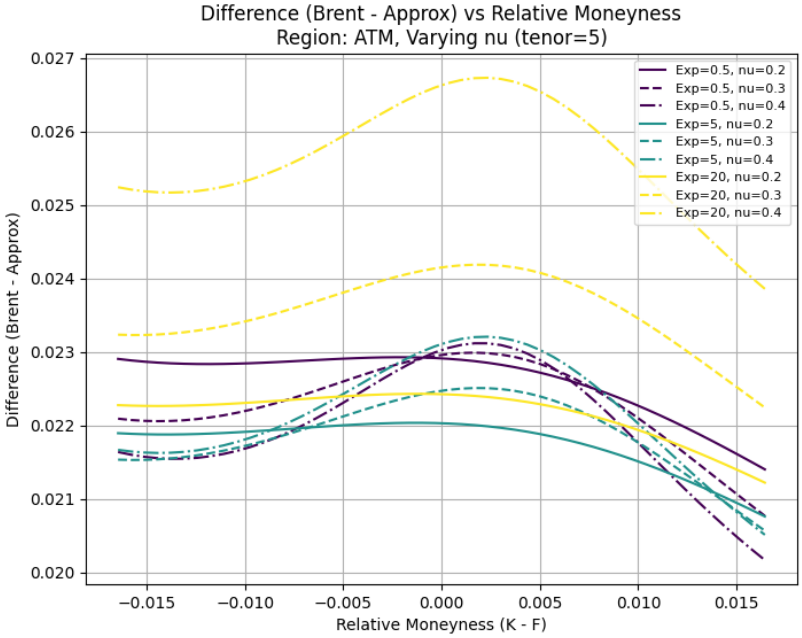
Difference (Brent - Approx) vs Relative Moneyness
Region: ATM, Varying nu (tenor=5)
Exp=0.5, nu=0.2
Exp=0.5, nu=0.3
Exp=0.5, nu=0.4
Exp=5, nu=0.2
Exp=5, nu=0.3
Exp=5, nu=0.4
Exp=20, nu=0.2
Exp=20, nu=0.3
Exp=20, nu=0.4
Difference (Brent - Approx)
Relative Moneyness (K - F)
0.027
0.026
0.025
0.024
0.023
0.022
0.021
0.020
−0.015
−0.010
−0.005
0.000
0.005
0.010
0.015

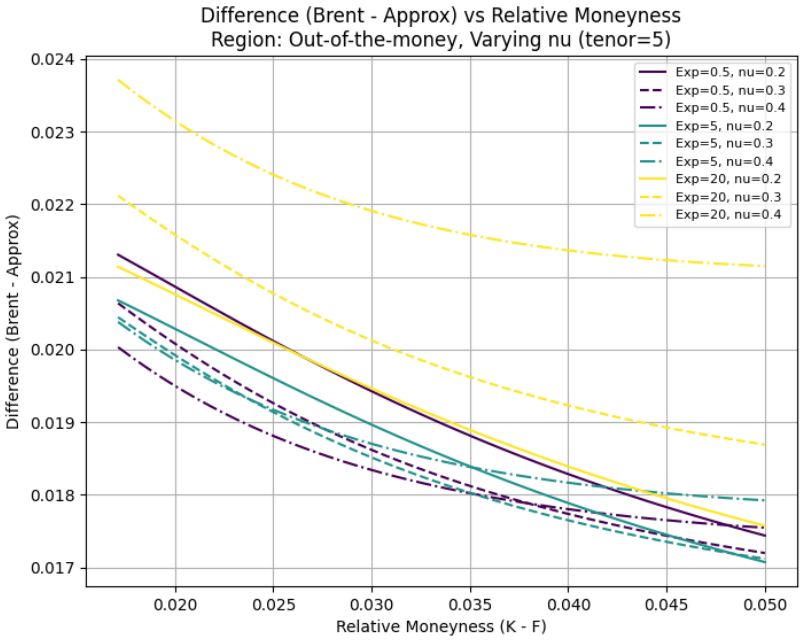
Difference (Brent - Approx) vs Relative Moneyness
Region: Out-of-the-money, Varying nu (tenor=5)
Exp=0.5, nu=0.2
Exp=0.5, nu=0.3
Exp=0.5, nu=0.4
Exp=5, nu=0.2
Exp=5, nu=0.3
Exp=5, nu=0.4
Exp=20, nu=0.2
Exp=20, nu=0.3
Exp=20, nu=0.4
Difference (Brent - Approx)
Relative Moneyness (K - F)
0.024
0.023
0.022
0.021
0.020
0.019
0.018
0.017
0.020
0.025
0.030
0.035
0.040
0.045
0.050

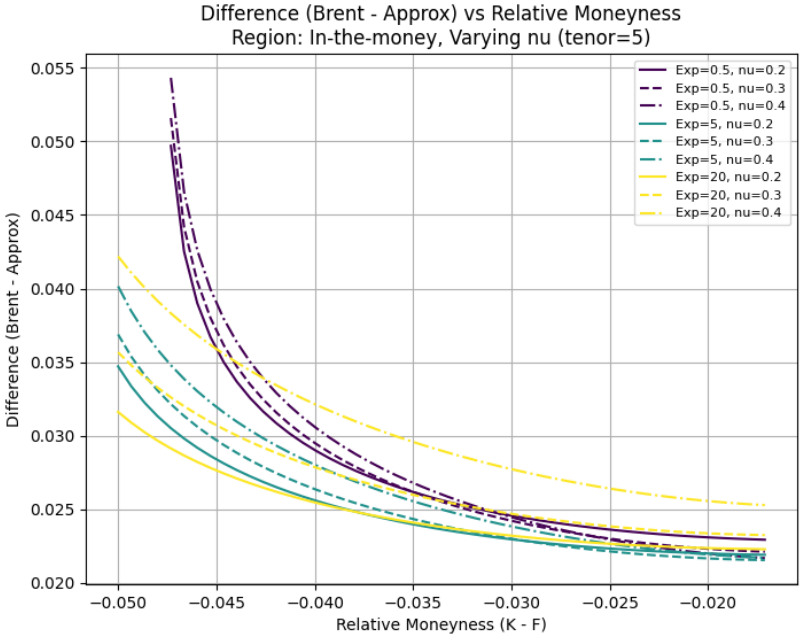

Varying ρ. The correlation parameter ρ shifts the skew orientation. Figures with $\rho \in \{-0.5, -0.3, -0.1\}$ show that negative correlation can create a steeper skew on the left side (ITM for payers), often increasing $\Delta\sigma_{\text{SLN}}$ in that region. Meanwhile, less negative ρ values yield a more moderate slope, typically reducing differences in the deep ITM. Overall, ρ changes can produce quite a spread in $\Delta\sigma_{\text{SLN}}$, indicating that if the approximate method or Brent-based method calibrates ρ differently, the wing mismatch can be substantial.

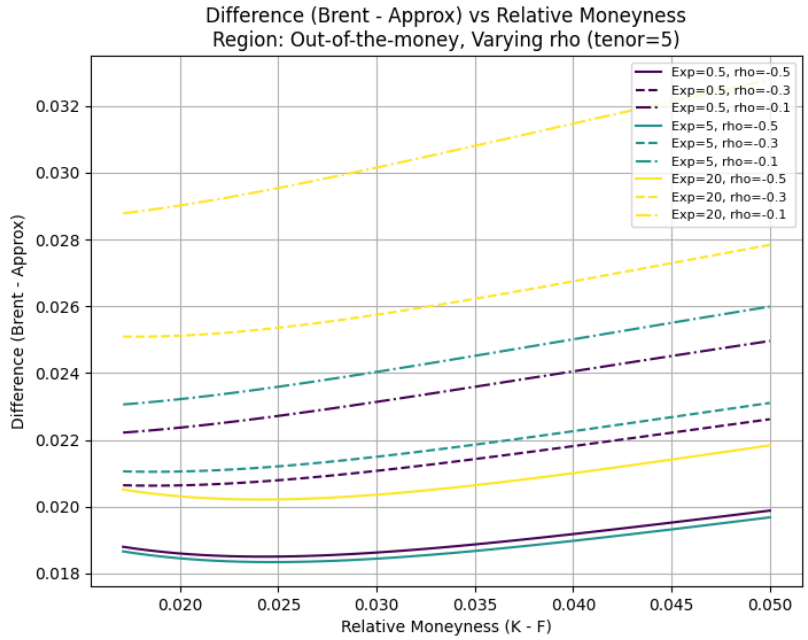
Difference (Brent - Approx) vs Relative Moneyness
Region: Out-of-the-money, Varying rho (tenor=5)
Exp=0.5, rho=-0.5
Exp=0.5, rho=-0.3
Exp=0.5, rho=-0.1
Exp=5, rho=-0.5
Exp=5, rho=-0.3
Exp=5, rho=-0.1
Exp=20, rho=-0.5
Exp=20, rho=-0.3
Exp=20, rho=-0.1
Difference (Brent - Approx)
0.032
0.030
0.028
0.026
0.024
0.022
0.020
0.018
0.020
0.025
0.030
0.035
0.040
0.045
0.050
Relative Moneyness (K - F)

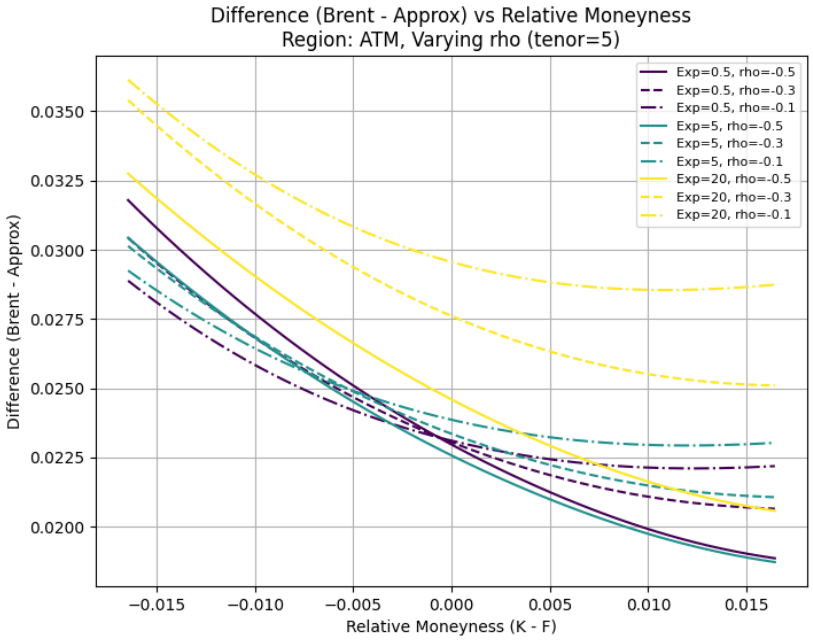
Difference (Brent - Approx) vs Relative Moneyness
Region: ATM, Varying rho (tenor=5)
Exp=0.5, rho=-0.5
Exp=0.5, rho=-0.3
Exp=0.5, rho=-0.1
Exp=5, rho=-0.5
Exp=5, rho=-0.3
Exp=5, rho=-0.1
Exp=20, rho=-0.5
Exp=20, rho=-0.3
Exp=20, rho=-0.1
Difference (Brent - Approx)
0.0350
0.0325
0.0300
0.0275
0.0250
0.0225
0.0200
−0.015
−0.010
−0.005
0.000
0.005
0.010
0.015
Relative Moneyness (K - F)

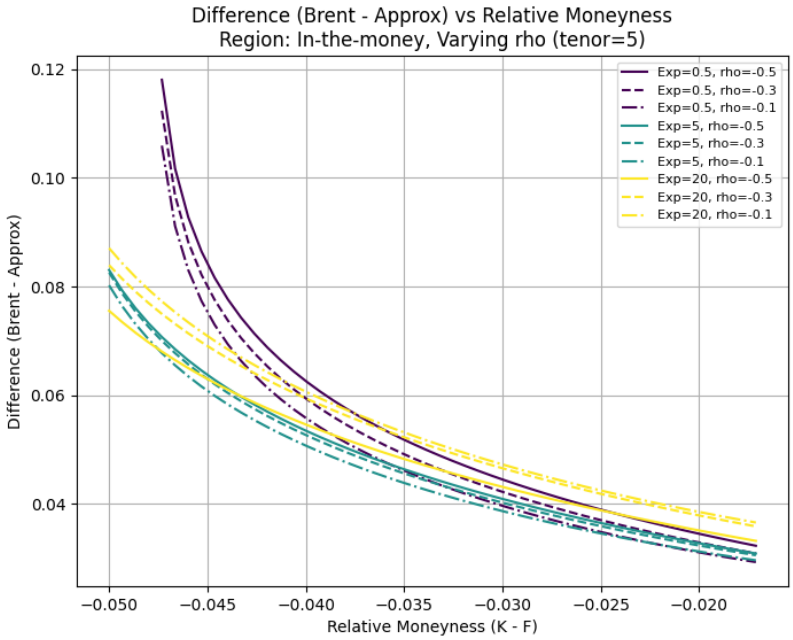

Varying λ (Shift). Finally, we vary the shift $\lambda \in \{0.05, 0.07, 0.09\}$. The shift ensures $F + \lambda$ and $K + \lambda$ remain positive, influencing how the log-moneyness transforms. In the plots, a larger shift generally reduces the relative effect of small changes in $F - K$, thus the difference $\Delta\sigma_{\text{SLN}}$ can become smaller near ATM but slightly larger in the deep ITM or OTM region. We also note that for longer expiries, a larger shift may cause the difference to be more uniform across strikes.

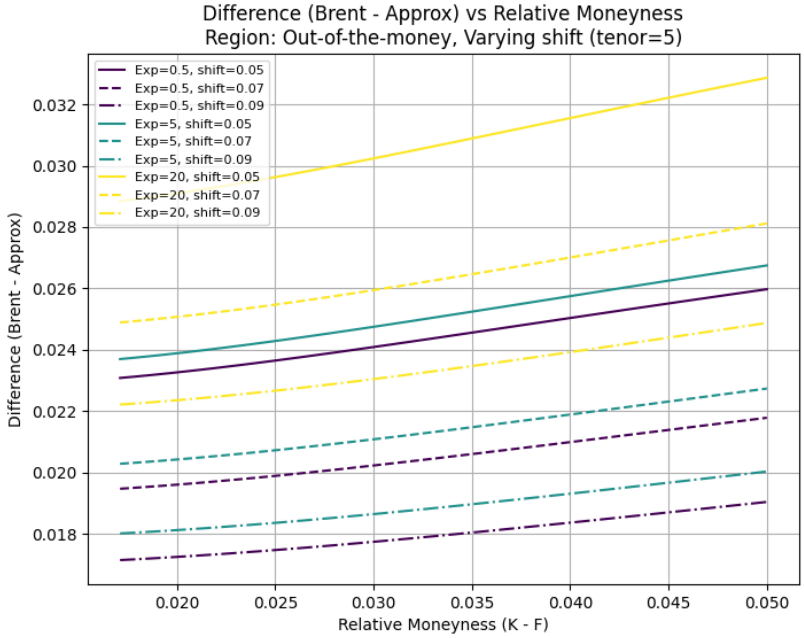
Difference (Brent - Approx) vs Relative Moneyness
Region: Out-of-the-money, Varying shift (tenor=5)
Exp=0.5, shift=0.05
Exp=0.5, shift=0.07
Exp=0.5, shift=0.09
Exp=5, shift=0.05
Exp=5, shift=0.07
Exp=5, shift=0.09
Exp=20, shift=0.05
Exp=20, shift=0.07
Exp=20, shift=0.09
Difference (Brent - Approx)
0.032
0.030
0.028
0.026
0.024
0.022
0.020
0.018
0.020
0.025
0.030
0.035
0.040
0.045
0.050
Relative Moneyness (K - F)

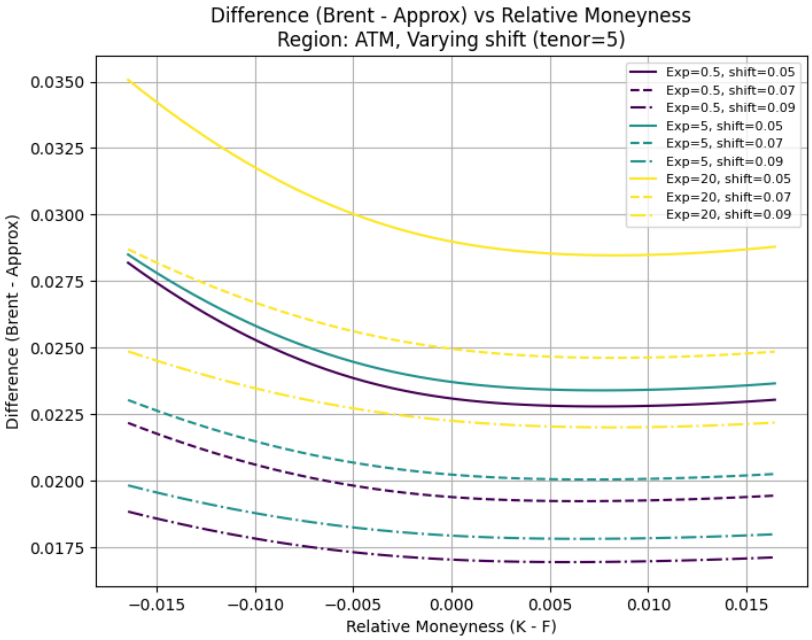
Difference (Brent - Approx) vs Relative Moneyness
Region: ATM, Varying shift (tenor=5)
Exp=0.5, shift=0.05
Exp=0.5, shift=0.07
Exp=0.5, shift=0.09
Exp=5, shift=0.05
Exp=5, shift=0.07
Exp=5, shift=0.09
Exp=20, shift=0.05
Exp=20, shift=0.07
Exp=20, shift=0.09
Difference (Brent - Approx)
0.0350
0.0325
0.0300
0.0275
0.0250
0.0225
0.0200
0.0175
−0.015
−0.010
−0.005
0.000
0.005
0.010
0.015
Relative Moneyness (K - F)

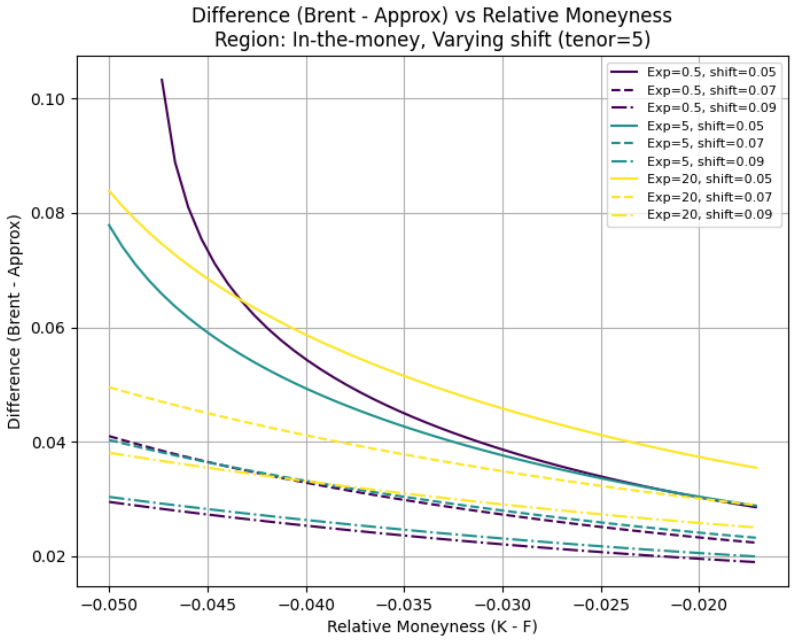

9.3 Key Takeaways

- **ATM Region:** Across all parameters, $\Delta\sigma_{\text{SLN}}$ remains comparatively low at or near ATM, indicating that both the Brent-based approach and the approximate approach align well for near-the-money options.
- **ITM & OTM Regions:** The most pronounced differences arise in the wings, where each parameter's effect on skew and curvature is magnified. Higher α or ν, or more negative ρ, tends to enlarge these discrepancies.
- **Expiry Dependence:** Short expiries ($T = 0.5$) often show larger mismatches in the wings, since small changes in parameters can have a bigger impact on near-term implied vol. Conversely, at very long expiries ($T = 20$), differences accumulate over time, also causing noticeable offsets.
- **Shift Influence:** Adjusting λ can mitigate or amplify wing differences, as it changes the effective scale of $F - K$. Larger shifts tend to flatten the difference near ATM but can push the mismatch outward to deeper ITM/OTM strikes.

Overall, these results confirm that σ_{SLN} and σ'_{SLN} can differ by a few basis points to well over 10 basis points, depending on the parameter in question, the region of moneyness, and the expiry. While the two methods agree fairly

well near ATM, practitioners should be mindful that any mismatch in SABR parameters (especially ν or ρ) or the chosen shift λ can lead to larger deviations in the far wings.

References

[1] P. Hagan, D. Kumar, A. Lesniewski, D. Woodward, *Universal Smiles*, Wilmott, Issue 84, Jul. 2016.